Resonant boron acceptor states in semiconducting diamond

S. G. Pavlov,[1] D. D. Prikhodko,[2,3] S. A. Tarelkin,[2,3,4] V. S. Bormashov,[4] N. V. Abrosimov,[5] M. S. Kuznetsov,[2]
S. A. Terentiev,[2] S. A. Nosukhin,[2] S. Yu. Troschiev,[2,4] V. D. Blank,[2,3] and H.-W. Hübers[1,6]

[1]*Institute of Optical Sensor Systems, German Aerospace Center (DLR), 12489 Berlin, Germany*
[2]*Technological Institute for Superhard and Novel Carbon Materials (TISNCM), Troitsk, 142190 Moscow, Russia*
[3]*Moscow Institute of Physics and Technology (National Research University), Dolgoprudny, 141701 Moscow Region, Russia*
[4]*The All-Russian Research Institute for Optical and Physical Measurements, 119361 Moscow, Russia*
[5]*Leibniz-Institut für Kristallzüchtung (IKZ), 12489 Berlin, Germany*
[6]*Institut für Physik, Humboldt-Universität zu Berlin, 12489 Berlin, Germany*

High-excited discrete states of boron hydrogenlike acceptors in crystalline diamond have been measured by temperature-dependent infrared absorption spectroscopy. We distinguish the boron resonant states in diamond crystals from the localized boron states in the band gap by differentiating the impurity transitions within state continua of the valence light- and heavy-hole subbands on the basis of their relative oscillator strengths, specific selection rules, and temperature dependences. Constraints on the boron binding energy and spin-orbit splitting of the valence band have been derived by analysis of the structure of the infrared absorption spectra of boron-doped diamond, in particular by a comparison with boron spectra in other semiconductors with a diamond lattice.

I. INTRODUCTION

The energy spectra of electrically active impurity centers in semiconductors emerge from a set of wave functions of electronic states in the minima of the related conduction or valence band. The energy states of the impurity occur as atomlike discrete spectra bound to the related band minima, below and above the extremum of the related band [1]. In *p*-doped semiconductors with a diamond-type (cubic) lattice, the lowest impurity states occur in the semiconductor band gap. The higher states, bound to the bands, are shifted upwards due to spin-orbit interaction (SO). In some cases, they merge with the continua of low-lying bands. These discrete impurity states are scattered within the light- and heavy-hole (lh-, hh-) valence subbands, in the energy gap between the bottoms of the SO subband and the degenerate lh-, hh-subbands (Fig. 1). They are called "resonant impurity states" [1,2]. In earlier publications, they were also called "internal impurity states" [3]. Resonant impurity states have been predicted theoretically for acceptors in several elemental semiconductors [2], but they were experimentally detected only in the case of shallow acceptors in silicon [3,4], and not for other cubic or zinc-blende semiconductors.

The knowledge of the resonant impurity spectra in cubic semiconductors is of particular interest for several reasons.

First, these spectra can be used for an estimation of the valley splitting due to SO interaction in semiconductors [5], and by this, for the SO coupling strength of the semiconductor. The eigenenergies of resonant states were used as empiric fitting parameters for the trial electronic wave functions in the variational calculations of impurity spectra of shallow acceptors in silicon (Si) and germanium (Ge) [2,6,7]. Obviously,

impurity resonances in the valance band may have an impact on electronic transport and optical properties.

In a uniaxially stressed *p*-type semiconductor, resonant states may occur in the energy gap between the bottoms of the stress-induced, split-off light- and heavy-hole subbands, and they may have a specific influence on charge-carrier scattering processes. This was observed for stressed Ge doped by gallium (Ga) [8]. Stimulated THz emission due to transitions involving such resonant states in stressed Ge:Ga [8] indicates extended lifetimes of charge carriers in the resonant states if compared with free holes. This was explained by a "coherent capture"-type inelastic scattering of holes into resonant states, which can be considered as resonant traps [9].

Boron, whose atoms act as electrically active acceptors at substitutional sites of cubic semiconductors, is currently the only element that allows for a comparative study of resonant acceptor states in elemental semiconductors with different ratios of the SO energy and the binding energy of an acceptor (Table I).

There is not yet a theory of boron electronic states in diamond explaining the experimentally observed infrared (IR) absorption spectra. The effective mass approximation (EMA) for the calculation of the energy spectrum of resonant acceptor states [2] is not directly applicable. Certain analogies to hydrogenlike spectra (see Fig. 1 for a sketch of the boron energy structure in diamond) can be drawn from the knowledge of resonant states in other semiconductors with a diamond-type band structure (Table I). These theories predict the energy spectra of odd-parity resonant states in *p*-Si and *p*-Ge to be mostly of mixed type constructed from contributions of the Γ_8 subband [mixed lh and hh subband(s), also referred to as $p_{3/2}$ bands due to their pseudo-angular momentum, $J = 3/2$]

TABLE I. Characteristic energies of elemental semiconductors doped by boron, as from Ref. [10]. The contribution of the valence-band subbands to the resonant state wave function is as predicted in [2]. Estimated values of the boron effective energy Ry* [11] that exceed the experimentally observed E_B are not shown. Entries marked with an asterisk were extrapolated using calculations for other shallow acceptors in Ge in [2].

| | Spin-orbit splitting (meV) | | | | Characteristics of the ground (1s) and odd-parity excited (np′) $p_{1/2}$ states of H-like acceptors [2] | |
	of the valence band, Δ	of the boron GS, Δ_B	Ry* (meV)	E_B (meV)	Localization of the $p_{1/2}$ states of boron	Contributions in the $p_{1/2}$ states of H-like acceptor
C	6(1) [12] 13 [13]	2.07(1) [14]	98 [15] 190 [16] 251 [11] 310 [17]	368 [16] 368.5 [18] 372 [14] 382 [17]	1s: band gap [14] np′: band gap [19]	
Si	43.5(3) [20] 44.00(2) [4] 44.1(4) [3] 44.6 [10]	22.751(2) [21]	24.46 [2]	45.63 [10]	1s: band gap [4] np′: resonant [3]	1s : $p_{1/2} \sim 50\%$ np′ : $p_{1/2} \sim 98\%$
Ge	296 [22] 290 [10]		4.31 [2] 4.355 [7]	10.805 [10]	1s: resonant [*] np′: resonant [*]	1s : $p_{1/2} \sim 95\%$ np′ : $p_{1/2} > 97\%$

and of the Γ_7 subband (SO subband, or $p_{1/2}$ band, $J = 1/2$) [2,10]. The discrete $p_{1/2}$ acceptor states become linked to the $p_{1/2}$ band bottom while the discrete $p_{3/2}$ states become linked to the $p_{3/2}$ band bottom. Because of the large spin-orbit splitting, Δ, in Ge and Si, the transitions into the boron resonant states are expected to be (and this is proved for Si:B, Fig. 2) clearly separated in the IR absorption spectra. The excited $p_{1/2}$ acceptor energy spectra of Ge and Si are predicted to consist of only resonant states [2], while in p-Si their ground state is downshifted in the Si band gap (Table I). The $p_{1/2}$ lower even-parity excited states are expected to be dominantly of

$n\Gamma_7^+$ type, while the lower odd-parity states are of Γ_6^- and Γ_8^- types (using notation of the O_h group theory symmetry) [2]. For both Si and Ge, resonant states are expected to obey the main features of hydrogenlike dopants.

Experimental studies show a small SO splitting energy of the boron ground state in diamond with respect to the valence-band SO splitting, $\Delta_B < \Delta$, and a large ionization energy E_B (Table I). This leads to an almost complete overlapping of the $p_{3/2}$ and $p_{1/2}$ energy spectra and related intracenter transitions, and very likely to equally large partial contributions of $p_{3/2}$ and $p_{1/2}$ bands to all excited boron states. Both types of excited states can be found in the band gap of diamond and in the energy gap between the $p_{3/2}$ and $p_{1/2}$ subband extrema (Figs. 1 –3). This makes determination of the $p_{3/2}$ band bottom and of the SO energy in diamond challenging.

The theoretical investigation of the eigenenergies of the resonant states in cubic semiconductors predicts small oscillator strengths for IR transitions into resonant states. Compared to transitions within the band gap, they are at least one order of magnitude lower for Si:B, and at least two orders of magnitude lower for hydrogenlike acceptors in Ge [2]. While resonant states in Si:B were found 60 years ago [3], this remains the only experimental evidence for such states of acceptors in unperturbed lattices of elemental semiconductors. This is partly due to technological difficulties in the production of both low- and moderately doped crystals with research grade quality, which are needed for such investigations.

We report on the observation of resonant impurity states in boron-doped single crystalline diamond, which has the smallest SO splitting of all elemental semiconductors and overlapping spectra of $p_{3/2}$ and $p_{1/2}$ related states. The differentiation between resonant states and states in the band gap of C:B was made based on the temperature behavior of the line intensities at the edge of the valence band. The analysis of the structure of ir absorption spectra of diamond doped with boron at different concentrations enabled constraints to be put on the boron binding energy and SO subband splitting.
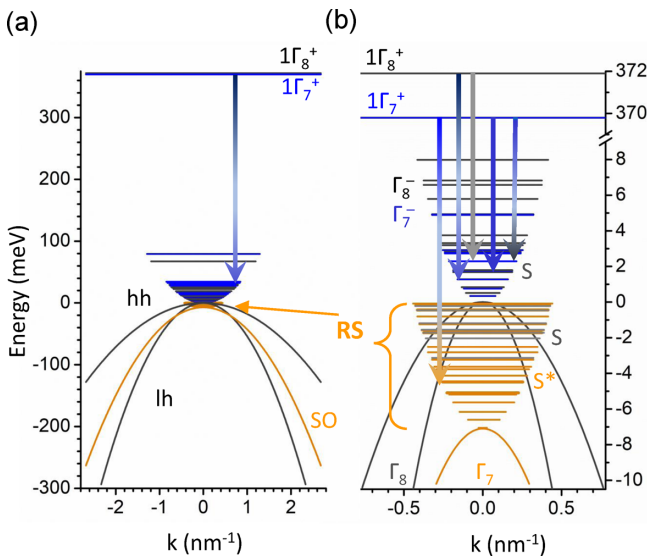
FIG. 1. Schematic presentation of the valence subbands (lh, hh, SO); localized and resonant (RS) impurity states of a boron acceptor in diamond (a), (b). The subband's bottoms are shown as having parabolic dispersion; see the text for further details. The solid arrows are experimentally observed impurity transitions.
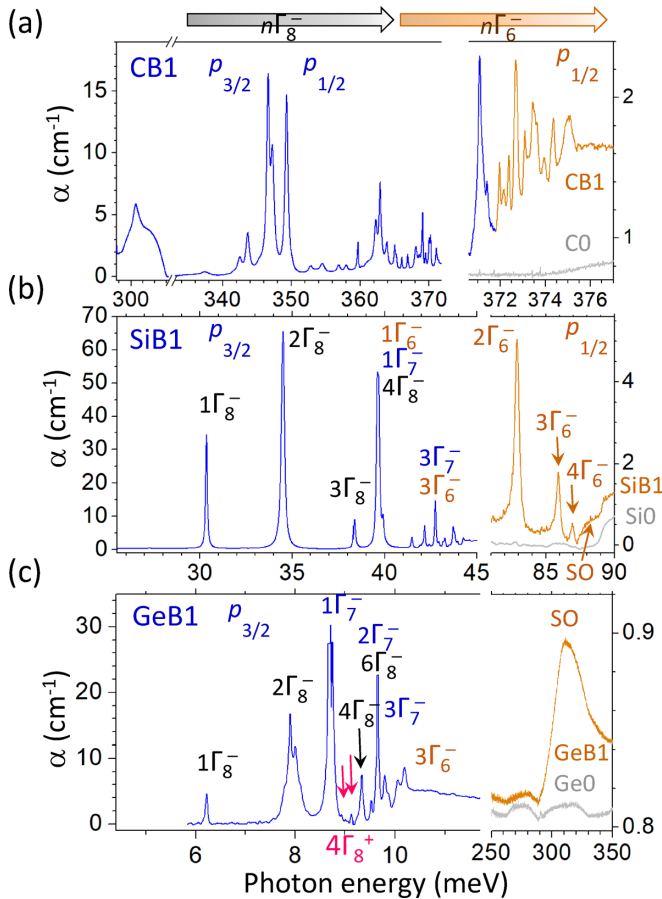
FIG. 2. Absorption spectra of boron doped and undoped semiconductors at 5 K [only transitions from the ground $1\Gamma_8^+$ ($p_{3/2}$) state are shown]: (a) diamond, (b) silicon, and (c) germanium samples, scaled by an $\sim Ry^{*2}$ factor. The right part of each plot shows spectral regions where transitions into the resonant states are expected. A few excited boron states corresponding to the most intense impurity lines are marked for Si and Ge. The tag SO indicates the spectral region in the vicinity of the $(E_B + SO)$ energy.

II. EXPERIMENT

The results of temperature-dependent infrared Fourier transform spectroscopy were used for analysis of the energy spectra of boron-doped crystalline diamond.

A. Sample preparation and characterization

Up to now, boron has been the only technologically feasible and controllable dopant in diamond (C:B), independent of growth and doping technologies. Large synthetic C:B crystals with low lattice defect density can be produced, for instance, by the temperature gradient method under high-pressure, high-temperature conditions (HPHT) with the simultaneous doping of diamond by boron in solid form from the melt [23]. The unavoidable compensation by residual nitrogen donors is supposed to play a dominant role for line broadening in HPHT bulk diamonds. Diamonds grown by chemical vapor deposition (CVD) do not have such high nitrogen concentrations, but they suffer from line broadening due to commonly occurring lattice defects.

We used a series of low- to moderately doped [$\sim (1$–$30) \times 10^{16}$ cm^{-3}] single-crystal diamonds (C:B) grown at the Technological Institute for Superhard and Novel Carbon Materials (TISNCM) by the temperature gradient method under high-pressure, high-temperature conditions with doping by natural boron (about 20% of ^{10}B and 80% of ^{11}B in C : ^{nat}B) or isotopically enriched boron (up to 99% with ^{11}B in initial boron oxide B_2O_3) from the melt. Until now, absorption spectra of low-doped, high-quality synthetic diamonds with isotopic enrichment of boron revealed the best resolved series of boron transitions in the vicinity of the valence-band bottom [24]. From the top (opposite to the seed) of the plane of the large grown crystals, parallel (001)-oriented plates were laser-cut. The plates were then wedged to $\sim 1°$ between the largest facets, and both large facets were polished with optical quality. Special diaphragms were prepared in order to limit the propagation of infrared light through homogeneously boron-doped sectors [determined by the size of (001) sectors in plane], as determined by UV-excited photoluminescence. The concentration of donors, compensating boron (mainly residual nitrogen) in the diamond crystals, was estimated to not exceed 1×10^{15} cm^{-3}. The boron concentration was estimated based on a calibration using the integrated absorption coefficient of the acceptor line in the absorption spectra at 300 K [18]. The temperature-dependent absorption spectra were taken for the C : ^{11}B samples: (CB1; 385 μm thick) with an uncompensated boron concentration of about 1.8×10^{16} cm^{-3}, and (CB2; 287 μm thick) with an uncompensated boron concentration of about 6.5×10^{16} cm^{-3}. Other samples with isotopically enriched C : ^{11}B and natural boron C : ^{nat}B up to concentrations of 3×10^{17} cm^{-3} were used explicitly for the determination of the photoionization energy (see the details below). An undoped IIa diamond sample (C0) has been prepared for reference spectra, using the same technology as for the doped samples but without adding boron into the melt.

Silicon and germanium crystals, doped by boron simultaneously from the melt, using gas doping with diborane (B_2H_6) [25], were used for preparation of the samples for comparative spectral measurements. Two samples were made from boron-doped germanium (GeB1, 3-mm-thick, 2° wedged, boron: 5×10^{14} cm^{-3}) and silicon (SiB1, 0.8-mm-thick, 1.5° wedged, boron: 3×10^{15} cm^{-3}) crystals, while the undoped Si (Si0) and Ge (Ge0) samples of the same geometry were used for the reference spectra to underline lattice absorption in these semiconductors.

B. Infrared absorption spectroscopy

Temperature-dependent IR absorption spectroscopy was performed using a Bruker Vertex 80v IR Fourier-transform spectrometer equipped with a helium-flow cryostat from Janis. The temperature of the cryostat's cold finger, as measured by a pair of attached thermosensors, was varied from room temperature down to 5 K. The C:B samples were attached to an intermediate copper holder and were covered by a mask with a central rectangular opening with a size of about the measured (001) sector, typically 2×2 mm^2. The holders were fixed to the cold finger with thermally conductive silver paint. The resolution of the spectrometer was varied in the range of 0.1–0.5 cm^{-1} (photon energy: 12.4–62.0 μeV). The measured

FIG. 3. Typical absorption spectra of boron doped (sample CB2) and undoped diamond (C0) at different lattice temperatures: at $T \sim 5$ K only boron transitions from the acceptor ground state $1\Gamma_8^+$ ($p_{3/2}$) are present, while at $T > 20$ K additional transitions from the SO ground state $1\Gamma_7^+$ ($p_{1/2}$) occur. Note the enhanced strengths of discrete transitions with the photon energy above 371 meV at elevated temperatures. The scales of optical density (OD) for the left and right parts of the absorption spectra are different. For clarity, the spectra are shifted vertically.

spectra were calibrated to the two-phonon absorption bands of the undoped IIa diamond.

The transmission spectra were taken at temperatures from 5 to 150 K (Fig. 3). The typical spectra of a boron-doped diamond sample (Figs. 2 and 3) present several types of impurity intracenter transitions: the strongest lines observed at $T = 5$ K in the spectral range below 370 meV correspond reasonably well to transitions of the following type: ground state $1\Gamma_8^+(p_{3/2}) \rightarrow$ odd-parity $n\Gamma_8^-(p_{3/2})$, $n\Gamma_7^-(p_{3/2})$ excited states (we will use the abbreviations $8^+_{3/2} \rightarrow 8^-_{3/2}$ or $7^-_{3/2}$ for such transitions in the following text), if the photon energy is scaled by a $\sim$Ry^{*2} factor (Table I); because of the large uncertainty of Ry* for boron in diamond (Table I), the C:B spectrum in Fig. 3 is scaled by a factor of 7 to the one of Si:B.

At lattice temperatures above ~ 20 K, additional boron transitions, originating from the thermally populated SO ground state $1\Gamma_7^+$ ($7^+_{1/2}$), accompany the impurity absorption spectra (Fig. 3). We will refer to the boron transition "pairs" originating from different ground states, $8^+_{3/2} \rightarrow S$ ($T > 5$ K) and $7^+_{1/2} \rightarrow S$ ($T > 18$ K), into the same excited boron state (S) as "parent" transitions.

There are several features indicating the different nature of transitions terminating in the excited boron states in the diamond band gap (localized acceptor states) and, possibly, in the $p_{3/2}$ state continuum (i.e., into resonant acceptor states).

First, for our analysis we assume that the SO splitting of the boron ground state is $\Delta_B = 2.07(1)$ meV as derived from Raman spectroscopy of C:B [14]. With this number, the "parent" transitions originating from $8^+_{3/2} \rightarrow S$ (at $T = 5$ K) and $7^+_{1/2} \rightarrow S$ (at $T > 20$ K) into presumably the same excited boron state (S) have a shift of about 0.015(5) meV for a transition energy below 370 meV, and of about 0.065(5) meV for a transition energy above 370 meV (Table II). While the first value can be assigned to a temperature-mediated shift of boron (S) states, the larger value of the shift together with the enhanced intensity indicates a change of the final transition state to the different (S^*) states, which are close in energy to some (S) states. We recall that the calculated energy spectra and intracenter transition strengths for Si:B and Ge:B [2,6,7] indicate the dominant $1\Gamma_8^+(p_{3/2}) \rightarrow n\Gamma_6^-(p_{1/2})$ type of tran-

sitions into resonant states. The redshifted transitions ending in the unresolved resonant states are composed of different symmetry combinations $k\Gamma_6^- + m\Gamma_7^- + n\Gamma_8^-$. They have the second largest oscillator strengths. Assuming a possible analogy in the spectrum of resonant boron states in diamond with its neighbors in the Periodic Table (Si,Ge), one may assume that the observed temperature-induced blueshifts of "parent" transitions and transitions with enhanced intensity above 370 meV indicate a significantly different symmetry of the excited states below and above this threshold energy. We note that no $8^+_{3/2} \rightarrow (S^*)$ transitions can be assigned in the low-temperature spectra (Fig. 4, Table II). This may cause specific selection rules, such as the following: The strongest $7^+_{1/2} \rightarrow (S^*)$ transitions occur into those excited states (S^*), into the strongest $8^+_{3/2} \rightarrow (S)$ transition occur or absent.

Next, in the spectral range above 371 meV, a significant increase of the $7^+_{1/2} \rightarrow (S/S^*)$ transition intensity occurs (Fig. 3). This increase can be explained assuming a significant extension of the boron state wave function within the binding-energy range $[0; -7.1]$ meV (Fig. 1) in the case of the stronger contribution of the OS subband (OS relative effective mass ~ 1.06) into these particular excited states (RS) in comparison to those within the diamond band gap (lh+hh relative effective mass of the density of states ~ 0.8).

Finally, the comparison of absorption cross-sections of differently doped diamond samples at $T = 5$ K (Fig. 5) with a simplified model for a hydrogenlike acceptor provided the binding energy of the boron acceptor in diamond E_B as about 371(1) meV. For this estimate, we used the analytical dependence of the optical cross-section on the photon excitation energy. This was derived for a hydrogenlike impurity center in the vicinity of the band extremum and applied to an acceptor–to–valence-band transition with parabolic dispersion [26,27], i.e., $\sigma(\hbar\omega) \sim (\hbar\omega - E_0)/(\hbar\omega)^5$ (dashed line in Figs. 4 and 5). We note here that such an approximation is limited by the assumed dispersion law, while complex anisotropy and nonparabolicity of the valence-band bottom were reported in theoretical studies; see, e.g., [11,13,15,17]. Our concluding estimate of the binding energy $E_B = 371.9(-1.2)$ meV is reasonably close to the value estimated from absorption spectroscopy by Kim *et al.* [14] (Table I).

TABLE II. Energies of the observed impurity transitions of the ^{11}B acceptor in diamond in the vicinity of the valence-band bottom and assigned types of the respective excited states. For weak transitions as well as for the lines on the steep slopes of a strong overlapping transition, an unambiguous determination was not possible. The "parent" transitions are listed in the same rows. MP denotes unresolved multiplet, listed in the same cells. The accuracy of the boron transitions is 0.012 meV; the absolute energies of boron resonant states are calculated assuming $\Delta = 7.1$ meV, $\Delta_B = 2.07$ meV, and $E_B = 371.9$ meV.

Boron absorption lines (meV) in the spectra:		Type of temperature dependence of the boron line	Boron state energy relative to the $p_{3/2}$ band bottom (meV)
OD@5 K	Δ_B shifted OD@20 K		
368.587 MP		$8^+{}_{3/2} \to p_{3/2}$	MP 3.31
369.061	366.911 MP	$8^+{}_{3/2} \to (S)_{3/2}$, $7^+{}_{1/2} \to (S)_{3/2}$	MP 2.839 / 2.819
	367.011 MP		MP 2.919
369.491 MP	367.436 MP	$8^+{}_{3/2} \to (S)_{3/2}$, $7^+{}_{1/2} \to (S)_{3/2}$	MP 2.409 / 2.394
369.578 MP	367.537 MP		MP 2.322 / 2.293
370.101 MP	368.072	$8^+{}_{3/2} \to (S)_{3/2}$, $7^+{}_{1/2} \to (S)_{3/2}$	MP 1.799 / 1.758
370.219 MP			MP 1.681
	368.555	$7^+{}_{1/2} \to (S)_{3/2}$ or $(S)_{1/2}$	1.275
371.064		$8^+{}_{3/2} \to (S)_{3/2}$ or $(S)_{1/2}$	0.836
	369.070	$7^+{}_{1/2} \to (S)_{3/2}$ or $(S)_{1/2}$	0.760
371.385		$8^+{}_{3/2} \to (8)_{3/2}$ or $(8)_{1/2}$	0.515
	369.486	$7^+{}_{1/2} \to (S)_{3/2}$ or $(S)_{1/2}$	0.344
371.982 MP			MP −0.082
372.120 MP		$8^+{}_{3/2} \to (S)_{1/2}$	MP −0.220
	369.993 MP	$7^+{}_{1/2} \to (S)_{1/2}$ or $(S^*)_{1/2}$	MP −0.163
372.361 MP		$8^+{}_{3/2} \to (S)_{1/2}$	MP −0.461
	370.275 MP	$7^+{}_{1/2} \to (S^*)_{1/2}$	MP −0.445
372.710		$8^+{}_{3/2} \to (8)_{1/2}$	−0.810
373.089		$8^+{}_{3/2} \to (S)_{1/2}$	−1.189
	371.078	$7^+{}_{1/2} \to (S^*)_{1/2}$	−1.248
373.453 MP		$8^+{}_{3/2} \to (S)_{1/2}$	MP −1.553
	371.409 MP	$7^+{}_{1/2} \to (S^*)_{1/2}$	MP −1.579
373.617 MP	371.553 MP	$8^+{}_{3/2} \to (S)_{1/2}$	MP −1.717
		$7^+{}_{1/2} \to (S^*)_{1/2}$	MP −1.723
373.937		$8^+{}_{3/2} \to (S)_{1/2}$	−2.037
	371.942	$7^+{}_{1/2} \to (S^*)_{1/2}$	−2.112
374.338		$8^+{}_{3/2} \to (S)_{1/2}$	−2.438
	372.346	$7^+{}_{1/2} \to (S^*)_{1/2}$	−2.516
	372.648	$7^+{}_{1/2} \to (S^*)_{1/2}$	−2.818
375.08		$8^+{}_{3/2} \to (S)_{1/2}$	−3.130
	373.066	$7^+{}_{1/2} \to (S^*)_{1/2}$	−3.236
	373.456	$7^+{}_{1/2} \to (S^*)_{1/2}$	−3.626
	373.598	$7^+{}_{1/2} \to (S^*)_{1/2}$	−3.768
	373.963	$7^+{}_{1/2} \to (S^*)_{1/2}$	−4.133
	374.316	$7^+{}_{1/2} \to (S^*)_{1/2}$	−4.486
	374.925 MP	$7^+{}_{1/2} \to (S^*)_{1/2}$	MP −5.095
	375.036 MP		MP −5.206
	375.460	$7^+{}_{1/2} \to (S^*)_{1/2}$	−5.630
	375.988	$7^+{}_{1/2} \to (S^*)_{1/2}$	−6.158
	376.433	$7^+{}_{1/2} \to (S^*)_{1/2}$	−6.603
	376.885	$7^+{}_{1/2} \to (S^*)_{1/2}$	−7.055
$p_{3/2}$ bottom	371.9 (−1.2)		0
$p_{1/2}$ bottom	379 (+1)		7 (1)

The boron states with the $8^+{}_{3/2}$ (or $7^+{}_{1/2}$) $\to$ $(S)_{1/2}$ or $(S^*)_{1/2}$ transition energies above 371.9 meV (369.83 meV) are, therefore, resonant relative to the $p_{3/2}$ band (Table II). The spectrum of resonant states in the $p_{3/2}$ band

continuum consists of the n series with at least one pair of states with wave functions having a symmetry (S), favorable for a larger oscillator strength of np' transitions originating from the ground $1\Gamma_8{}^+ (p_{3/2})$ state, while it consists of another
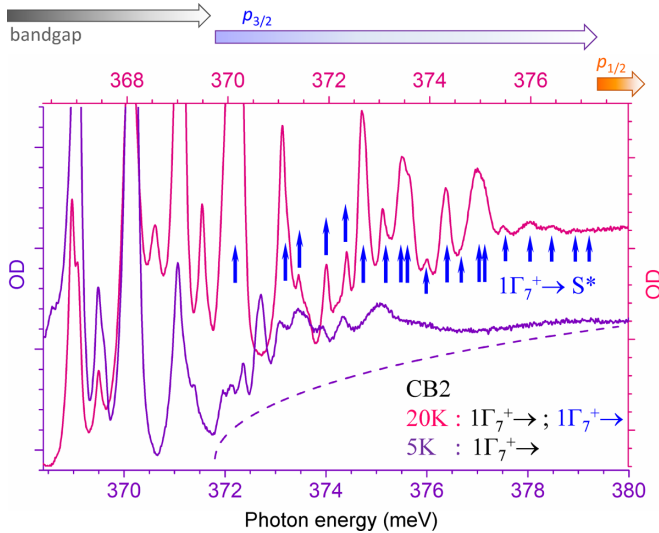
FIG. 4. Spectrally resolved discrete transitions in the vicinity of the valence-band edge in the absorption spectra of boron doped diamond (CB2 sample); amplitudes are given in optical densities (OD) and shifted for clarity: (violet) absorption spectrum OD ($\hbar\omega - \Delta_B$) taken at 5 K; (pink) absorption spectrum at 20 K OD ($\hbar\omega - \Delta_B$), shifted by Δ_B, so that the $8^+_{3/2} \to S$ and $7^+_{1/2} \to S$ transition series in the same excited boron state are spectrally matched. Vertical arrows indicate the positions of the boron transitions ($\to S^*$) with the abnormally enhanced strengths at $T > 20$ K. The dashed line shows the approximate boron impurity to the $8^+_{3/2} \to p_{3/2}$ band continuum absorption spectrum.

series with wave functions having a symmetry (S^*), favorable for a larger oscillator strength of np' transitions originating from the ground $1\Gamma_7^+(p_{1/2})$ state.
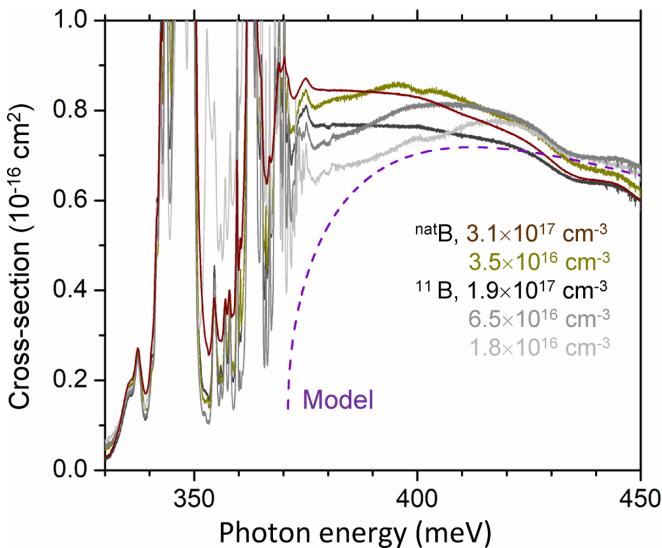
FIG. 5. Cross-section of several samples with different boron (natural isotopic content ^{nat}B and isotopically enriched ^{11}B) concentrations in the vicinity of the boron binding energy at $T = 5$ K. The model of the ionization cross-section for a hydrogenlike acceptor yields a value of the ionization energy $E_B \geqslant 371(1)$ meV for a boron center in diamond.

To put constraints on the $p_{1/2}$ band extremum, and thus on the SO splitting in diamond, we return first to the spectra of boron-doped Ge and Si, having the same diamond-type lattice and a similar valence-band structure. In Si:B and Ge:B, the $p_{1/2}$ band extremum can be assigned to a clear spectral feature, a specific broadband (SO in Fig. 2), commonly observed in doped Si and Ge (SiB1 and GeB1), but not appearing in the undoped reference samples (Si0 and Ge0). It fits very well to the reported values of the ($E_B + SO$) energy (Table I). While in Ge:B such a feature could include the spectrally unresolved $8^+_{3/2} \to$ transitions into densely spaced resonant boron states, it does not strongly affect the accuracy of the SO energy in Ge. For Si:B, it exceeds certainly the intensity of the $8^+_{3/2} \to np'$ transitions into high $n > 4$ resonant boron states, predicted to be an order magnitude weaker [2]. A similar spectral feature is missing in all measured spectra of our C:B crystals. Furthermore, strong defect-induced phonon spectral features are inherent for doped diamond [14]. They indicate a strong electron-phonon coupling of impurities and phononic excitation, and they hinder a clear assignment of broad spectral features in relevant regions. The ($E_B + SO$) energy fits into the relatively strong multiphonon band, which can be seen in the three-phonon absorption band of the C0 sample above 374 meV [Fig. 2(a)]. One of the potential attributes for the $p_{1/2}$ band extremum is the convergence of the discrete boron lines, which occurs above the energy of ($\hbar\omega + \Delta_B$), where $\hbar\omega = 376.885$ meV is the highest-energy resolved $7^+_{1/2} \to (S^*)_{1/2}$ boron transition. This provides the estimate for the $p_{1/2}$ band extremum as 379 (+1) meV and SO splitting in diamond $\Delta = 7(1)$ meV. It is in good agreement with the value derived from cyclotron resonance measurements [12] (Table I).

At above $\sim$375 meV, the boron transitions occur exclusively at temperatures providing significant thermal population of the SO ground state, $1\Gamma_7^+$. The strength of these transitions drops significantly when compared with those in the range of resonant states with larger binding energy. We do not have an explanation for this behavior. As was stated in some theoretical works, resonant states can be potentially found in continua of semiconductors and not necessarily related to degenerate and liftoff/multisubband energy spectra [1]. However, no experimental evidence of such materials has been reported yet.

III. CONCLUSIONS

The observation of resonant states of the boron acceptor in diamond has a few challenges:

(i) The complex structure of the valence band in the vicinity of its extrema, resulting in strong admixing of SO-split subbands to the wave function of all excited boron states. This causes large similarities between states related to different subbands. Several attempts to develop a theory of boron states in diamond did not lead to a successful model explaining the observed impurity spectra.

(ii) Spectrally close transitions into localized and scattered (resonant) boron states. Spectral resolution of individual transitions requires a tradeoff between samples with low concentration broadening and detectable absorption at low oscillator strengths.

(iii) Technological challenges for obtaining research-grade boron-doped diamonds with relatively low concentrations of uncompensated boron in crystals with high-quality lattices.

The latter was the main reason that experimental research on possible resonant states of boron in diamond was not pursued for a long time. This also restricted the attempts to assign experimental values to parameters such as the binding (ionization) energy of an acceptor, for instance. The widely used determination of ionization energies of hydrogenlike impurities in elemental semiconductors is based on adding the theoretical binding-energy value to the experimentally determined transition energy from the ground impurity into a particular excited state. This state should, on the one hand, be resolved in absorption spectra, and on the other hand it should be possibly close to the EMT predicted wave function and binding energy. For an acceptor in Si, this is the $1\Gamma_8^+ \rightarrow 8\Gamma_8^-$ transition which is added to the theoretical value of the binding energy of the excited $8\Gamma_8^-$ state, 2.69 meV [10]. For an acceptor in Ge, it is the $1\Gamma_8^+ \rightarrow 2\Gamma_8^-$ transition and the binding energy of the excited $2\Gamma_8^-$ state, 2.8673 meV [7].

Because no theoretical spectrum of boron in diamond is available, we used the following experimental findings obtained from low-temperature ir absorption spectra for such an analysis:

(i) Convergence of the discrete spectrum of intracenter transitions of a boron acceptor.

(ii) Relative strengths of impurity transitions in the vicinity of the valence-band edge and selection rules for the transitions originating from the $p_{3/2}$- and $p_{1/2}$-type boron ground states, which indicates changes of the type of the symmetry of the final states.

(iii) Slope of the absorption cross-section for differently doped diamond crystals, accounting for a typical photoionization dependence on photon energy in the vicinity of the valence-band extrema.

(iv) Analogy of the analysis of the determination of ionization energy and resonant states of boron in other semiconductors with a diamond-type lattice structure, and available theoretical energy spectrum of boron states.

The derived estimates for the $p_{3/2}$ and $p_{1/2}$ band extrema, $E_B = 371.9(-1.2)$ meV and 379 $(+1)$ meV, and for the orbit splitting in diamond, $\Delta = 7(1)$ meV, are in fair agreement with the values derived from cyclotron resonance measurements [$\Delta = 6(1)$ meV [12]], from infrared absorption ($E_B = 372$ meV [14]), and from photoionization spectroscopy ($E_B = 368.5$ meV [18]).

The spectra of resonant states of a hydrogenlike boron acceptor in diamond provide key data for comparison with similar spectra of resonant states in other elemental semiconductors. The resonant states of boron exhibit a large series of up to 20 resolved lines (possibly with another fine structure of states), much more than, for example, in Si:B where it is only three ($n = 2, 3, 4$). This is due, first of all, to the large binding energy of the boron acceptor in diamond, allowing us to spectrally resolve its exaggerated infrared spectrum, but it is also due to the specific structure of the levels, which strongly deviates from a Rydberg-type spectrum [2] as predicted for resonant states in p-Si and p-Ge. These specific features must be considered when developing a theory of boron states in diamond.

[1] F. Bassani, G. Iadonisi, and B. Preziosi, Rep. Prog. Phys. **37**, 1099 (1974).

[2] R. Buczko and F. Bassani, Phys. Rev. B **45**, 5838 (1992).

[3] S. Zwerdling, K. J. Button, B. Lax, and L. M. Roth, Phys. Rev. Lett. **4**, 173 (1960).

[4] D. W. Fischer and J. J. Rome, Phys. Rev. B **27**, 4826 (1983).

[5] Z. Yu, Y. X. Huang, and S. C. Shen, Phys. Rev. B **39**, 6287(R) (1989).

[6] I. L. Beinikhes, Sh. M. Kogan, M. G. Novak, and A. F. Polupanov, Mater. Sci. Forum **65–66**, 259 (1991).

[7] Yu. A. Kurskii, Phys. Rev. B **48**, 5148 (1993).

[8] I. V. Altukhov, M. S. Kagan, K. A. Korolev, V. P. Sinis, E. G. Chirkova, M. A. Odnoblyudov, and I. N. Yassievich, J. Exp. Theor. Phys. **88**, 51 (1999).

[9] M. A. Odnoblyudov, I. N. Yassievich, V. M. Chistyakov, and K. A. Chao, Phys. Rev. B **62**, 2486 (2000).

[10] B. Pajot, *Optical Absorption of Impurities and Defects in Semiconducting Crystals: I. Hydrogen-like Centres* (Springer, Berlin, 2010).

[11] M. E. Mora-Ramos, Phys. Status Solidi B **234**, 481 (2002).

[12] C. J. Rauch, in *Proceedings of the International Conference on the Physics of Semiconductors, Exeter, UK, 1962*, edited by A. C. Strickland(Institute of Physics and the Physical Society, London, 1962), p. 276.

[13] M. Willatzen, M. Cardona, and N. E. Christensen, Phys. Rev. B **50**, 18054 (1994).

[14] H. Kim, R. Vogelgesang, A. K. Ramdas, S. Rodriguez, M. Grimsditch, and T. R. Anthony, Phys. Rev. B **57**, 15315 (1998).

[15] I. L. Eremets, Semicond. Sci. Technol. **6**, 439 (1991).

[16] V. K. Bashenov, A. G. Gontar, and A. G. Petljkhov, Phys. Status Solidi B **108**, K139 (1981).

[17] E. Gheeraert, S. Koizumi, T. Teraji, H. Kanda, and M. Nesládek, Phys. Status Solidi A **174**, 39 (1999).

[18] A. T. Collins and A. W. S. Williams, J. Phys. C **4**, 1789 (1971).

[19] P. A. Crowther, P. J. Dean, and W. F. Sherman, Phys. Rev. **154**, 772 (1967).

[20] F. Evangelisti, A. Frova, M. Zanini, and E. O. Kane, Solid State Commun. **11**, 611 (1972).

[21] K. J. Morse, R. J. S. Abraham, D. P. Franke, N. V. Abrosimov, and M. L. W. Thewalt, Phys. Rev. B **93**, 125207 (2016).

[22] M. V. Hobden, J. Phys. Chem. Solids **23**, 821 (1962).

[23] V. S. Bormashov, S. A. Tarelkin, S. G. Buga, M. S. Kuznetsov, S. A. Terentiev, A. N. Semenov, and V. D. Blank, Diam. Relat. Mater. **35**, 19 (2013).

[24] D. D. Prikhodko, S. G. Pavlov, S. A. Tarelkin, V. S. Bormashov, M. S. Kuznetsov, S. A. Terentiev, S. A. Nosukhin, S. Yu. Troschiev, H.-W. Hübers, and V. D. Blank, Phys. Rev. B **102**, 155204 (2020).

[25] R. R. Sumathi, N. V. Abrosimov, K.-P. Gradwohl, M. Czupalla, and J. Fischer, J. Cryst. Growth **535**, 125490 (2020).

[26] B. K. Ridley, *Quantum Processes in Semiconductors*, 4th ed. (Oxford University Press, New York, 1999), p. 201.

[27] P. W. Banks, S. Brand, and M. Jaros, J. Phys. C **13**, 6167 (1980).